

# **THE PORTABLE SIX-AXIS-ARM 3D MEASURING SYSTEM: PRECISE METROLOGY APPLICATIONS FOR EXPERIMENTAL EQUIPMENT AT GANIL**

*Rémy Beunard, GANIL<sup>1</sup>, BP55027, 14076 Caen, Cedex5, France*

## **ABSTRACT**

We will present in this paper two experimental installations in which the portable measuring system plays its full part as a “3D Surveyor”. In the first application we will give comments on the measurement of the mechanical structure of the gamma-ray spectrometer. The geometrical parameters of the germanium detectors placed around the target will be analysed. The second application describes measurement, in a reaction chamber, of a multi-detector with strips. The unit is made up of eight independent telescopes of which the first element is a  $60 \times 60$  mm silicon detector. The aim of the measurement is to know the three-dimensional position of each silicon detector in the Cartesian reference frame of the target.

## **1. INTRODUCTION**

Three-dimensional measurement methods, with or without contact with the measured object, still vary widely, but the choice of measuring system must meet the accuracy requirements as well as being appropriate for the circumstances of the experiment.

The purpose of this article is to demonstrate the benefits of the portable six-axis-arm system for measurements of equipment being built for nuclear physics experiments. Our choice of this device was governed both by the complex geometry of the objects involved and by the extremely unfavourable environment for the use of conventional instrumentation.

This instrument enables the survey of points in three dimensions ( $X, Y, Z$ ) by means of a contact sensor. The accuracy specifications supplied by the manufacturer are of course related to the design of the system but they also depend on the space being measured. The measurement accuracy is being continually improved. Based on the length test (see Section 3) values range from  $\pm 0.018$  mm ( $2\sigma$ ) for the most accurate measurements, to  $\pm 0.17$  mm ( $2\sigma$ ) for the worst.

Apart from these aspects of quality, the makers have produced valuable innovations in terms of ergonomics. The full rotation of the joints offered by some manufacturers is a notable advance which simplifies the use of the arm, especially in confined spaces.

In this article we give details of two experimental installations in which the portable measuring system plays its full part as a “3D Surveyor”. Various possible solutions were

---

<sup>1</sup> GANIL: National heavy-ion accelerator facility (Grand Accélérateur National d'Ions Lourds)

considered, including employing an outside contractor, with all the resulting inconvenience such as the difficulty of planning the work and the need to obtain permits to work in controlled areas (INB<sup>2</sup> zones), and the alternative of hiring the measuring equipment. The latter was adopted, with the aim of proceeding to a full trial.

## 2. MEASURING PRINCIPLE

We will not give technical details of the design of this instrument which go beyond our expertise, but it will be helpful to review certain principles.

This very versatile measurement system was designed for portability and maximum stability. It may be rigidly attached in a variety of ways to the objects being measured, or it may be mounted on a movable tripod. The six axes of rotation of the arm allow it to be used in many different positions. The end of the arm is equipped with a sensor which supplies the 3D coordinates of the point of contact, directly after the observation is validated. The special feature of the system is the opportunity for remote control of the position of the measuring mark of the computer by the operator. The software linked with the arm allows direct processing of geometrical entities such as straight lines, planes, cylinders, etc. The data can be exported to Autocad<sup>®</sup> design software or compared with the CAD model produced from CATIA<sup>®</sup> files.

## 3. DEFINING THE ACCURACY OF MEASURING ARMS

Confusion frequently arises when the accuracy of such portable measurement systems is discussed [1]. To improve clarity, some designers' technical documentation may indicate the different tests carried out, usually by measurement of a set of points following different approach vectors in relation to a sphere or a cone. However, in these two tests the movements of the arm are relatively small. A better assessment would undoubtedly be obtained by measuring points between two spheres within the range of measurement of the arm. It is sufficient to measure the distance between two points while varying their position as well as the distance between the spheres. In this case the arms are required to operate in variable positions and orientations and therefore in conditions closer to those encountered in practical use.

## 4. MEASUREMENT OF THE MECHANICAL STRUCTURE OF THE GAMMA-RAY SPECTROMETER [2]

EXOGRAM (EXOtiques GAMma) is the name of GANIL's experimental apparatus for the detection of gamma rays (Fig. 1). It consists of 16 detectors which use extremely pure germanium crystals assembled in a very compact geometrical array (Fig. 4). The apparatus is designed to study the structure of atomic nuclei, which is one of the main lines of fundamental research at GANIL. It detects and measures the energy of gamma-ray photons. To identify and/or study the products of reactions, the detectors are placed around the target (Fig. 2). One of the characteristics of germanium detectors is their excellent energy resolution, which permits detailed and precise studies of the nuclei being investigated. Under certain reaction mechanisms the recoil velocity of the nucleus emitting gamma-rays may be large, which results in a substantial Doppler broadening effect. This can lead to a deterioration of the energy resolution of

---

<sup>2</sup> INB : Basic nuclear installation (Installation Nucléaire de Base)

the measured rays as well as a displacement of the observed peaks. To correct the latter effect, it is essential that the angular positions of the detectors around the target are accurately known.

#### 4.1 Measurement of the mechanical structure of the gamma spectrometer – the problem

The aim was to acquire as-built 3-dimensional data about the whole array in order to deduce the geometrical parameters rho, theta and phi ( $\rho$ ,  $\theta$ ,  $\varphi$ ) for the germanium detectors placed around the target. These parameters are of course linked to the geometry of the array but

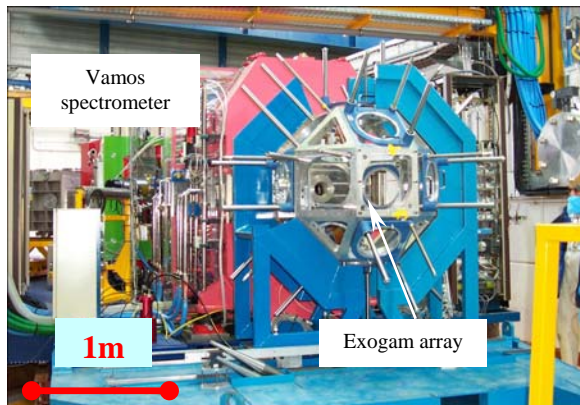


Figure 1: Mechanical structure of the EXOGAM array linked to the VAMOS spectrometer

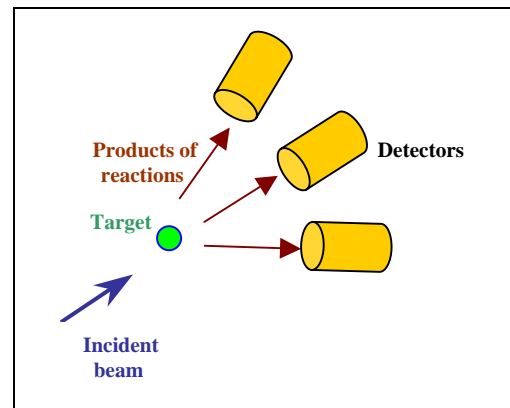


Figure 2: Diagram showing the principle of the detection system

they depend especially on the mechanical adjustment of the movable housings on their guide rods (Fig.4).

As it was impossible to measure the detectors directly because of their inaccessibility, it was decided to compute their positions from knowledge of the geometry of their movable housings, this being an essential part of the determination of their final coordinates. In the course of an experiment the detector can move in a straight line defined by two points on the normal to the movable housing at its centre. These two points correspond to the extreme positions of the detector on the guides. The physicist required first of all to know the orientations  $\theta$  and  $\varphi$  of the detectors in relation to the target to  $\pm 0.2^\circ$ , a value which corresponds to the angle subtended by an object with diameter of 0.7 mm at a distance of 100 mm from the target. This distance is approximately the closest possible position of a detector in relation to the target. For a constant angle, the diameter of the object varies in proportion to its distance from the target. If we consider this value of  $\pm 0.2^\circ$  to be the maximum permitted error, the standard deviation of the measuring instrument must not exceed  $\pm 0.35 \text{ mm} / 2.66$  or  $\sigma = \pm 0.13 \text{ mm}$ , assuming that errors of observation are normally distributed. For this task we hired a ROMER 3200 mm measuring arm with appropriate accuracy characteristics. The calibration report indicated an overall variance of  $0.0046 \text{ mm}^2$  for tests of precision and repeatability. The measuring accuracy is thus known from the length test to be  $\pm 0.14 \text{ mm}$  at the  $2\sigma$  level. It must be emphasised that in the final estimates of accuracy the manufacturer has included a temperature parameter, either by

providing each encoder with sensors or simply by elimination of adjustment errors through the use of very stable materials such as carbon graphite in the construction of the arm. The coefficient of expansion of this material is  $0.25 \times 10^{-6} \text{ m} / ^\circ\text{C}$  and this value did apply to the arm used in this case.

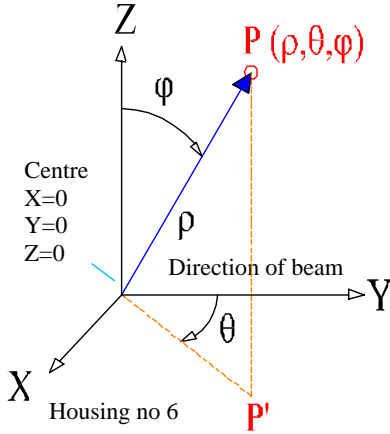


Figure 3: Coordinate system used

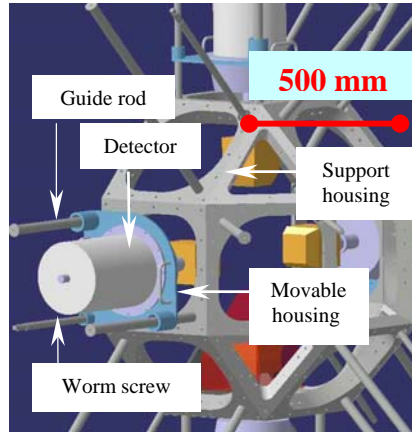


Figure 4: Exploded CAD view of the structure equipped with 4 detectors

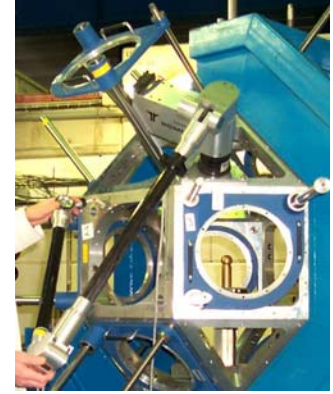


Figure 5: Attachment of the 6-axis measuring arm to the structure

## 4.2 Measurement of the mechanical structure of the gamma spectrometer – setting up the process

The chief difficulty was in the careful placement of the measuring arm within the structure (Fig.5) so as to limit the required number of stations to two. After initialising the axes and opening the files, the measuring operation could begin. At this stage a specific reference frame could be adopted, or that of the arm itself could be retained. The latter solution was adopted because it was then easier to use a 3D Helmert transformation from the arm system to the Cartesian coordinates of the target while holding fixed the axis of the beam between the centres of the entry and exit housings.

The movement of the arm is a rather complex operation because a single coordinate system must cover all the required points. To achieve this, theoretical (designed) coordinates are allocated to three points which have been measured previously. The software adjusts these values to the full set of measured points by minimising the discrepancies at every point. If the standard deviation exceeds the pre-set value (0.12 mm in our case) the measurement is rejected. The overall uncertainty within the space being measured, taking into account the movement of the arm, can be estimated as:

$$\sqrt{0.14^2 + 0.12^2} = \pm 0.18 \text{ mm} \quad (1)$$

This value of the measuring accuracy is entirely acceptable and lies within the requirements laid down in the technical specification. It translates into an angular accuracy of  $\pm 0.1^\circ$  for a detector placed 100 mm from the target.

### 4.3 Measurement of the mechanical structure of the gamma spectrometer – the object being measured

#### 4.3.1 Checking the geometry of the structure

The object to be measured consists of fixed housings assembled together so as to form a spherical framework. This first check enabled the geometry of the object to be defined and the correct assembly of the 18 housings to be verified. Their geometrical centres are defined by the measurement of points on each face and inside each bore (Fig. 6). Once the centre is computed, this is projected onto the plane face of the housing. At every stage we were able to monitor the progress of the measurements by means of the displayed  $\sigma$  value and cancel a measurement in case of anomalous results.

The final coordinates of the centre of the spherical structure emerge from a computation based on measurement of all of the fixed housings. The mean value obtained for the parameter  $\rho$  was 483.08 mm against a theoretical (design) value of 482.84 mm. The maximum angular errors recorded for  $\theta$  and  $\varphi$  respectively were  $-0.06^\circ$  and  $+0.08^\circ$ . These values indicate that the object as built is very close to its theoretical design (see Table 1 – part only shown here).

#### 4.3.2 Three-dimensional measurement of the internal bore of the movable detector housings

The three-dimensional position of each movable germanium detector housing was measured at its two extreme positions on its supporting guide rods (Fig. 7). The principle of the measurement described in the previous section was again used here. The maximum angular

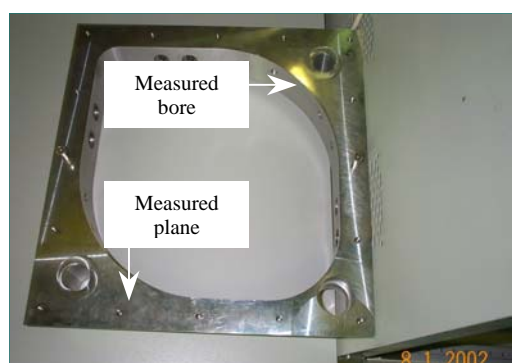


Figure 6: View of a fixed housing

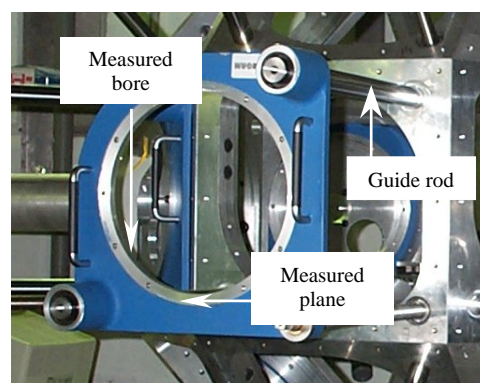


Figure 7: View of a movable housing at the outer limit of its movement along the guide rods

discrepancies from theoretical values recorded at the centre of the movable housing were  $+0.06^\circ$  and  $+0.07^\circ$  for  $\theta$  and  $\varphi$  respectively. These are similar to the values found in the measurement of the main structure itself, thereby indicating that the guide rods are correctly positioned on the structure.

### 4.3.3 Computation of the three-dimensional positions of the detectors from knowledge of the geometry of the movable housings

The sensitive portion of the detector corresponds to a calculated point on the line normal to the centre of the movable housing at a distance of 390 mm. Table 2 (part only given here) provides us with spherical coordinates of each point, calculated from the centre of the structure. If the faces of the movable housings were exactly parallel to the fixed housings, we would find the same angles  $\theta$  and  $\varphi$  as those measured at the time of checking the main structure itself (vectors collinear). The analysis of the full set of data allows us to deduce a small rotation of the movable housings. However, we note in Table 2 that the largest discrepancies occur at the front (inner) positions. The problem was investigated and found to be due to a mechanical constraint

Object Centre of fixed housing	$\rho$ (m)	$\theta^\circ$ clockwise	$d\theta$ from theoretical value	$\varphi^\circ$	$d\varphi$ from theoretical value
1	0.48302	359.940	- 0.06	44.992	-0.008
2	0.48299	225.003	+ 0.003	89.996	-0.004
3	0.48325	134.954	- 0.046	89.977	-0.023
4	0.48295	179.987	- 0.013	44.984	-0.016
5	0.48326	90.000	0	90.000	0
...					

Table 1: Results of measurement of 3D positions of fixed housings (part of table) (all angles in degrees and decimals)

Object Theoretical position of detector	$\rho$ (m)	$\theta^\circ$ clockwise	$d\theta$ from theoretical value	$\varphi^\circ$	$d\varphi$ from theoretical value
Norm 1 front	0.1044	0.087	+ 0.087	45.124	+0.124
Norm 1 back	0.4416	359.927	-0.073	45.067	+0.067
Norm 2 f	0.1044	224.919	-0.081	89.838	-0.162
Norm 2 b	0.4523	224.995	-0.005	89.884	-0.116
Norm 3 f	0.1049	135.242	+0.242	90.303	+0.303
Norm 3 b	0.4539	135.023	+0.023	90.028	+0.028
Norm 4 f	0.1048	180.069	+0.069	44.881	-0.119
Norm 4 b	0.4528	179.972	-0.028	44.945	-0.055
Norm 5 f	0.1043	180.153	+0.153	134.659	-0.341
Norm ...					

Table 2: Results of 3D computation of points on the normal to each housing (part of table) (all angles in degrees and decimals)

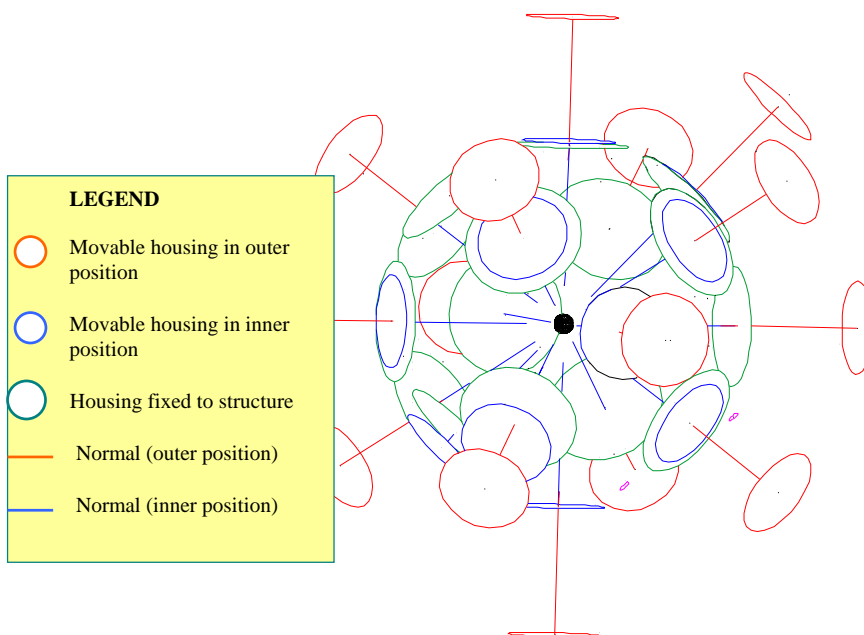


Figure 8: 3D drawing of the EXOGAM unit from measurements exported to Autocad<sup>®</sup> software via the IGES interface



on the worm screw as it approached the point of contact with the structure. This anomaly has been corrected.

## 5. MEASUREMENT OF THE MUST DETECTOR

MUST (MUR à STRips) is a silicon strip detector array for radioactive beam experiments (Fig. 9). It consists of eight independent telescopes. The first stage is a silicon strip detector with dimensions of  $60 \times 60$  mm and 300 microns thick, with 60 strips on each face arranged orthogonally, thus allowing horizontal and vertical positioning as well as a measure of energy. For energetic particles (for example protons of more than 6 MeV), the residual energy is measured in a Si(Li) detector 3 mm thick followed by a CsI crystal with a thickness of 15 mm read by a photodiode. Particles which pass through the first stage are identified by the loss of energy / energy method, slower particles by energy / time of flight measurements.

The MUST assembly was designed to be modular in order to be adaptable to different experimental configurations (Fig. 10). The columns can be placed either side by side with a minimal dead zone between the detectors, or in different parts of the beam. They are rigidly attached to the turntables in the SPEG<sup>3</sup> reaction chamber.

### 5.1 Measurement of the MUST detector – the problem

For about the past three years, the physicists have been expressing the desire for far more accurate knowledge of the 3D position of each of the silicon detectors around the target, in order to arrive at a much more precise analysis of the positions of particles in the detectors. Up to that time, the only measurement carried out on the detector in the reaction chamber was the geometrical location of the sides of the central module in relation to the theoretical trajectory of the beam. Data analysis was based purely on theoretical (designed) 3D coordinates. It quickly emerged that the detector assembly was not a perfect sphere; thus it became more and more difficult for the physicists to achieve a perfect reconstruction of the particle trajectories. It was

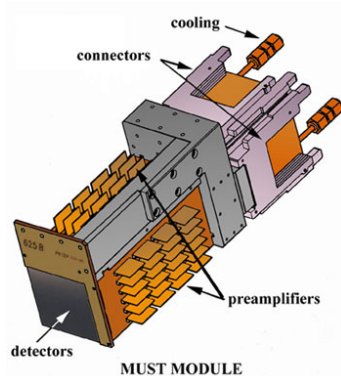


Figure 9: CAD view of one of the 8 telescopes of the MUST multi-detector

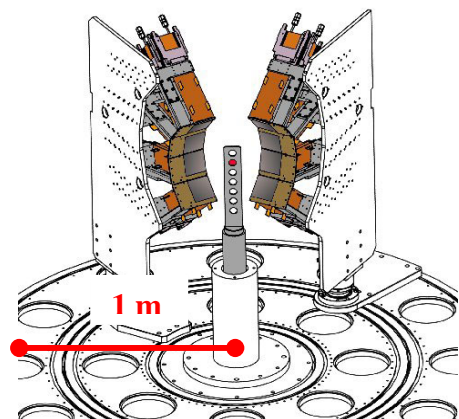


Figure 10: CAD view of one of the experimental configurations of the MUST assembly

necessary to find a metrological solution for the independent measurement of each detector in the Cartesian coordinate system of the target. The portable 3D measuring arm has satisfied this requirement.

We will now discuss the first stage of the silicon detector. This supplies both the position and the energy of the particle. The physicists wish to know the 3D positions of each silicon detector in the coordinate system of the target to an accuracy of better than half a strip-width, or  $\pm 0.20$  mm. This value has been retained as the maximum permitted discrepancy. This objective demands rigorous metrology. We hired a ROMER measuring arm with acceptable accuracy characteristics for a range of measurement of 2500 mm. The calibration report indicated an overall variance of  $0.0026 \text{ mm}^2$  for tests of precision and repeatability. The measuring accuracy is thus known from the length test to be  $\pm 0.10$  mm at  $2\sigma$ .

## 5.2 Measurement of the MUST detector – adding fiducial marks to the object in the laboratory

The fragility of the silicon detector forced us to insert fiducial marks into the printed circuit board (PCB). Obviously the arm could not be allowed to come into contact with the silicon itself. These marks were to become the real reference points for on-site measurements. It then remained for us to determine the 3D rectangular coordinates of the silicon detector in relation to these marks.

At the time of designing the detector, various inserts (calibrated holes) in the PCB were proposed in order to control the final assembly. As this has evolved over time, of the nine existing inserts only two are used to fix the PCB to the electronic module. The remaining inserts, by virtue of their design, have become useful reference marks for the precise positioning of the detector. These marks within the thickness of the PCB are small hollow copper cylinders thickly plated with gold (Fig. 11). The internal diameter of each cylinder is 3.0 mm. The geometry of the ends of the holes proved to be well suited to contact by means of a mechanical sensor.

Starting from this, a two-dimensional measurement of the silicon detector assembly was carried out in the laboratory by means of an XY table and a theodolite. For reasons of pointing accuracy, we favoured the sightings using the theodolite equipped with a panfocal telescope over

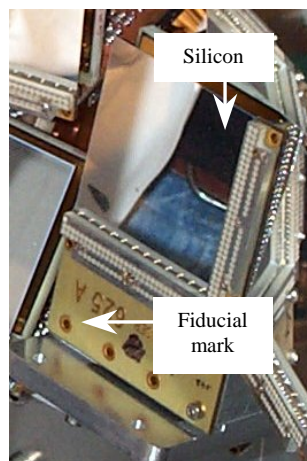


Figure 11: View of a silicon detector

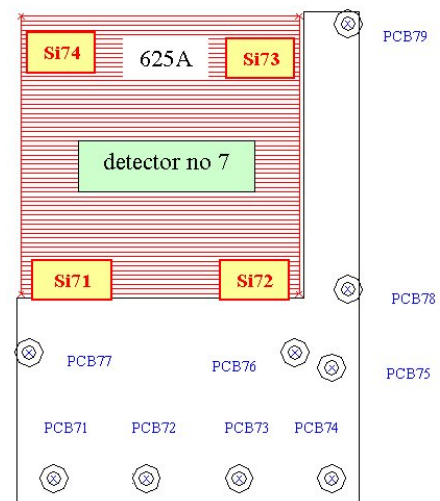


Figure 12: Drawing showing the numbering of the fiducial marks on the PCB

<sup>3</sup> SPEG : Ganil Energy Loss Spectrometer (Spectromètre à Pertes d'Énergie du Ganil)



those of the table lens. In this configuration, the detector was fixed vertically on the table. A first theodolite pointing to the centre of the first fiducial mark (PCB71) allowed the table to be reset and to display origin coordinates (0,0). The coordinates of other points (cylinders and corners of the silicon detectors) were given by successive measurements of the movement of the table in two orthogonal directions. The third dimension, that is the distance between the plane of the silicon and the face of the cylinders, was provided by means of a depth gauge.

The resulting error in the determination of the coordinates of the silicon detector relative to the PCB was evaluated to an accuracy of  $\pm 0.06$  mm by taking account of the movement of the table and the theodolite pointings.

### 5.3 Measurement of the MUST detector – setting up the process

The cylindrical structure of the reaction chamber consists of two connected components (Fig. 13). Where they meet, around the whole internal perimeter, are found the holes which among other functions allow a fixation of the measuring system in an ideal position in relation to the configurations of the experiments.

Before starting to measure the detectors, the first operation is to define a coordinate system (reference frame) (Fig. 14) in the reaction chamber for the duration of the measurements. The theoretical (designed) axis of the beam is indicated by a straight line defined by two reference marks. The first mark, inserted into the beam tube at the entrance to the reaction chamber, is removable in order to allow the beam itself to pass freely. The second mark is installed in a motorised set of slits at the exit from the reaction chamber. The target, which is placed in the centre of the reaction chamber, thus lies on the straight line already defined. These two points are aligned by means of a theodolite placed above them. Clearly these two marks are insufficient to

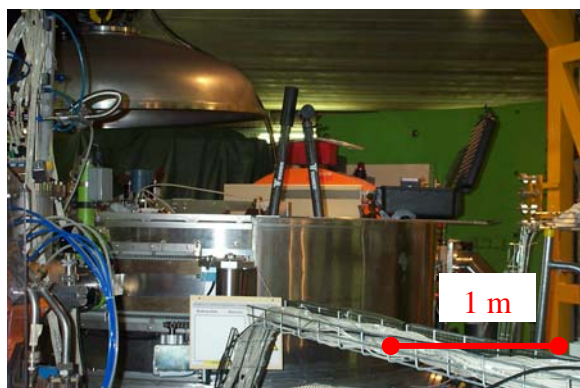


Figure 13: View of the reaction chamber in the experiment room of the SPEG spectrometer

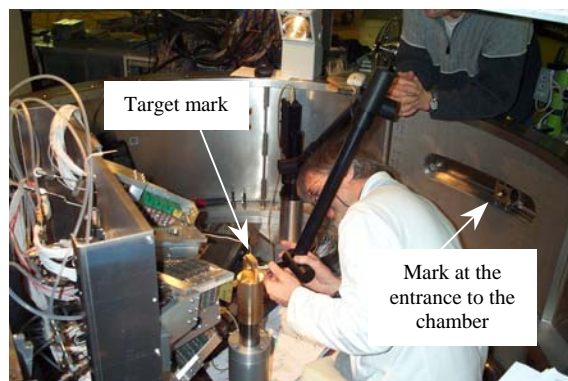


Figure 14: Metrology of the reference frame inside the reaction chamber

define the Cartesian coordinates of the object to be measured. A third reference mark, placed on the wall of the chamber and on another line at right angles to the first, provides orientation within the horizontal plane. The movement of the target carriers in the vertical plane provides supplementary dimensional information for the determination of the orientation of the object.

#### 5.4 Measurement of the MUST detector – the object to be measured in the reaction chamber

Inside the reaction chamber, having measured the reference framework, it is only necessary to measure the four closest fiducial marks attached to the PCB for each silicon detector (Fig. 15). To determine the 3D coordinates of each mark, we first need to define the plane of the face of the cylinders. This plane is determined by measuring several points on the ring by means of a stylus with a spherical tip 1.0 mm diameter (contact probe). The centre of the cylinder is obtained by measuring an adjusted point in the plane of the ring by contact with the base of the cylinder using a stylus of diameter 6.0 mm. As we know the relative coordinates of the PCB / detector assembly in the object reference system, it now suffices to carry out a 3D Helmert transformation from the old system (laboratory measurement) to the new system (measurement in the reaction chamber), computing the transformation parameters (scale, three rotations and three translations) to obtain the 3D coordinates of the four corners of each silicon detector in the Cartesian coordinate system of the target.



Figure 15: Measurement of fiducial marks on the MUST detector in the reaction

The root mean square error from the Helmert transformation is of the order of 0.09 mm for the arithmetic mean of the eight transformations. The overall uncertainty in the three-dimensional positions of the detectors in the reaction chamber can be estimated from the measuring accuracy of the instrument, the error resulting from the determination of coordinates of the detector relative to the PCB, the error in the Helmert transformation and the alignment error of the reference frame:

$$\sqrt{0.10^2 + 0.06^2 + 0.09^2 + 0.07^2} = \pm 0.16 \text{ mm} \quad (2)$$

no	dx mm	dy mm	dz mm	ρ mm	θ (clockwise)	φ	Distance check mm	Lab measurement mm	Remarks
PCB76	47.77	174.24	-94.94				57.37	57.44	fiducial marks
PCB77	-9.33	180.00	-97.31						
PCB78	58.92	176.62	-81.16				57.35	57.46	
PCB79	58.24	191.98	-25.91						
Si71	-11.09	184.94	-85.27	203.95	356.57	114.71	59.93	59.93	silicon detectors
Si72	48.48	178.94	-82.79	203.04	15.16	114.06			
Si73	47.65	194.81	-25.03	202.11	13.74	97.11	59.84	59.84	
Si74	-11.84	200.82	-27.43	203.03	356.63	97.76			
Calculated distance : PCB77-Si74 : 72.96 (lab measurement: 72.96)									
S.D.: 0.07 mm									

Table 3: 3D coordinates of the four corners of silicon detector no. 7 obtained by a 3D Helmert transformation (angles in degrees and decimals)

This value for the measurement error remains satisfactory and meets the requirements stated by the physicist in charge of the experiment. It can be translated into an angular discrepancy of  $\pm 0.06^\circ$  for a detector placed as close as possible to the target, that is at 150 mm. In their extreme positions, the MUST modules lie at a radius of 375 mm. As the uncertainty in measurement is not linked to the radius at which the detector is placed, the angular accuracy increases as a function of its distance from the target and translates into a discrepancy of  $0.02^\circ$  for a detector at a distance of 375 mm. The final result is given for each detector in the form of the root mean square error (Table 3).

## 6. CONCLUSION

The introduction of new technologies in our laboratories is necessary and allows significant improvements in metrology and thus even in the physics experiments themselves. We consider ourselves under an obligation to put forward a variety of methods rather than being restricted to a single approach. We must also remain very adaptable to the conditions on site.

The decision to use this measuring procedure for these two applications was quickly taken because the advantages compared with conventional surveying methods are obvious. Portability, flexibility and the time required were all decisive. A further advantage of the process is the use of a single instrument and thus a single observer to carry out the measurements. It should be noted that the system is restricted to small objects with dimensions of less than 5 m and with only a small number of points to be measured. Nevertheless, some manufacturers are now proposing a seventh linear axis in order to increase the volume which can be surveyed.

The accuracy values quoted by the manufacturers are very impressive. Nevertheless it would be interesting to measure an object using a variety of different three-dimensional metrology procedures and compare the results.

Through these two examples we have sought to demonstrate that the unconventional metrology equipment and processes employed on the GANIL experiments are well suited to the small dimensions of the objects involved. In order to achieve high quality results it is essential to involve the surveyor in the project planning and design, from the initial stages of defining the requirements and well ahead of the measurement itself. A broad appreciation of the problem enables the surveyor to supply the most suitable solution from among the tools already in the laboratory or available in the marketplace. His role on site must be followed up by providing advice to the physicist or the project manager during the analysis and use of the results.

## 7. RÉFÉRENCES

- [1]: « Précis » n'est pas assez précis ! Définition de la précision des bras de mesure- FARO News 1/2004, page 9
- [2]: R. Beunard, « Le système de mesure 3D portable à bras six axes dans la métrologie des accélérateurs de particules, un instrument adapté à la mesure de la géométrie du nouveau dispositif expérimental de détection de rayonnements gamma installé au GANIL », revue XYZ n° 95 éditée par l'AFT (Association Française de Topographie), juin 2003, pages 43-46